Supporting Information

Excited-State Reaction Dynamics of the Radical Anions Revealed by the Novel Time-Resolved Photofragment Depletion Spectroscopy

Sejun An and Sang Kyu Kim*

Department of Chemistry, KAIST, Daejeon (34141), Republic of Korea

*Corresponding author: sangkyukim@kaist.ac.kr

Table of Contents

1. Electron Affinities and Energy Diagram

We determined the electron affinities (binding energies) of species (states) involved in the dissociation pathways of nitromethane monomer and dimer anions through reference values or theoretical calculations. Electron affinities related to the $CH_3NO_2^-$ → CH_3 + NO_2^- reaction can be easily obtained from the references. According to the references, the electron binding energy of $CH_3NO_2^-$ is 0.17 eV,[2] 0.01 eV for NBS,[3] and NO_2^- for 2.3 eV[4]. For the dissociation reactions of the dimer anion, $(CH_3NO_2)_2$ is known to have an electron affinity of about 0.8 eV,[5] but there is no available data for NBS and $NO_2^-(CH_3NO_2)$. Generally, NBS exhibits a very weak electron binding energy. Even in the case of extremely large dipole moments, such as 20 D for $(NaCl)_2$, it does not exceed 0.2 eV.[6] Considering that a deviation of approximately 0.1 eV does not significantly impact the overall trend of our interpretation, we assumed the electron binding energy of NBS as 0.01 eV, consistent with the monomer case. The electron affinity of $NO_2(CH_3NO_2)$ was obtained through theoretical calculations. Observing that the structure is not optimized for the neutral state, it is presumed to possess a stable structure only in the anion form, undergoing a significant structure rearrangement upon electron detachment. Therefore, we determined the electron affinity by leveraging the fact that solvation-induced stabilization is negligible for the neutral state. This can be expressed in the following formula:

$$E_{CH_3NO_2} + E_{NO_2} \approx E_{NO_{2(CH_3NO_2)}}$$

$$Binding\ Energy_{NO_2^-(CH_3NO_2)} = E_{NO_2(CH_3NO_2)} - E_{NO_2^-(CH_3NO_2)}$$
$$= E_{CH_3NO_2} + E_{NO_2} - E_{NO_2^-(CH_3NO_2)}$$

The energies in last term, $E_{CH_3NO_2}, E_{NO_2}, and\ E_{NO_2^-(CH_3NO_2)}$ were calculated using B3LYP/6-311G++(3df, 3pd) method, resulting in a 2.9 eV for the electron affinity of the $NO_2(CH_3NO_2)$. Finally, the electron binding energy of the dimer anion in the vibrationally hot ground state (D_0^* state) is assumed to be slightly lower than 0.8 eV due to vibrational energy, which is plotted as 0.4 eV in the Fig. 3g.

The energy diagram in Fig. 4 was constructed based on experimental and theoretical results. The geometries for the ground state of nitromethane dimer anion and neutral were optimized using the B3LYP/6-311G++(3df, 3pd) method. The energy difference between D_0 state in the anion and neutral equilibrium geometry was calculated to 0.52 eV. Whereas, the excitation energies of the NBS were extracted from the photofragment action spectrum. Since NBS has a nearly identical structure with the neutral state, adiabatic and vertical excitation energies for the D_0 → NBS

transition can be identified from the appearance and maximum energy of the absorption spectrum. From the photofragment action spectrum, they were estimated as 0.8 and 1.6 eV, respectively. The vertical excitation energy for the $D_0 \rightarrow \sigma_{CN}^*$ state transition was predicted to be 1.65 eV from the TD-DFT calculation. The asymptotic energy of the σ_{CN}^* was estimated from the dissociation threshold calculation using B3LYP/6-311G++(3df, 3pd) calculation, which gives 0.82 eV.

2. Temperature Effect on the Nitromethane Dimer Anion

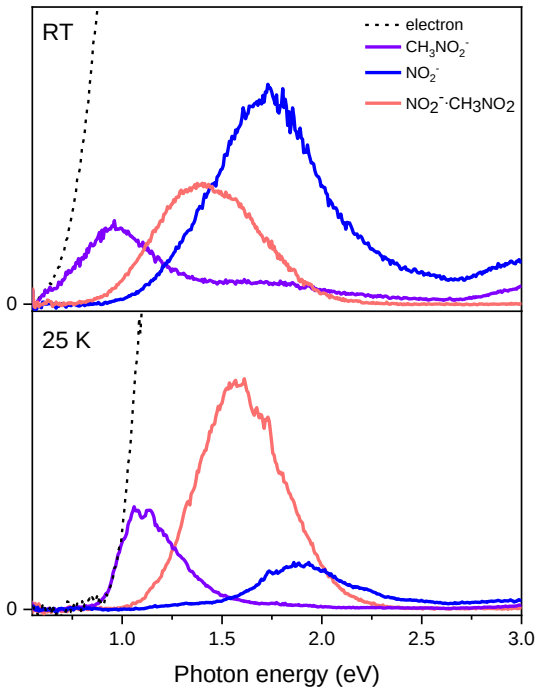

Fig. S1 Photodetachment and photofragment action spectra of room-temperature and reprinted[1] cryogenically cooled nitromethane dimer anion.

We obtained the photodetachment and photofragment action spectra of the nitromethane dimer anion at cryogenic and room temperature (Fig. S1). Similar to the cryogenically cooled nitromethane dimer anion reported in a previous study at 25 K,[1] the fragment yield signifies the absorption profile of NBS. While the overall absorption profile remains similar, broadening is pronounced at room temperature due to hot bands. $NO_2^-(CH_3NO_2)$ and NO_2^- fragment yield shows significant differences depending on the internal temperature of the parent ion. This discrepancy likely arises from the vibrational modes induced by the initial temperature of the parent anion, enhancing the internal energy of the fragment and facilitating additional cluster decomposition.

Hence, it is inferred that the initial temperature of the parent anion has minimal impact on the dissociation mechanism. Indeed, when obtaining time-resolved photodepletion (TRPD) spectra for the $NO_2^-(CH_3NO_2)$ fragment at both cryogenic and room temperatures, almost identical time constants and transient profiles were observed (Fig. S2). This implies that increasing the ion temperature to enhance the yield of NO_2^- for efficient acquisition of TRPD spectra had little impact on the dissociation dynamics.

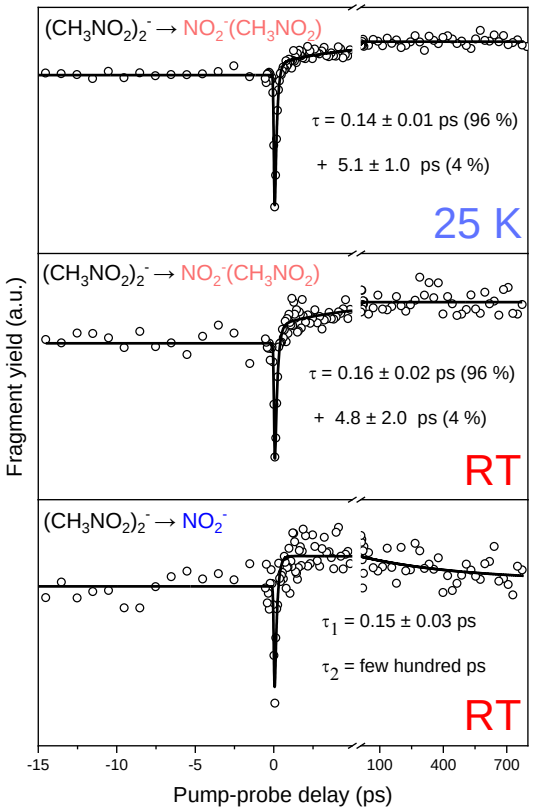

Fig. S2 TRPD spectra for $NO_2^-(CH_3NO_2)$ and NO_2^- fragments originating from $(CH_3NO_2)_2^-$ at cryogenic and room temperature. The transients for $CH_3NO_2^- \rightarrow NO_2^-(CH_3NO_2)$ with varying ion temperature exhibit nearly identical time constant and profiles.

3. Developing the Mathematical Model for the Transients

$CH_3NO_2^- \rightarrow CH_3 + NO_2^-$

In contrast to conventional time-resolved spectroscopy data, every state involved in the reaction pathway can influence the transients. Therefore, we developed a mathematical model to fit our experimental data. The bond cleavage reaction of monomer nitromethane anion is a relatively simple process, expressed as:

$$R \overset{hv}{\rightarrow} I\ (NBS) \overset{\tau}{\rightarrow} P\ (NO_2^-)$$

The fitting function for the fragment yield of this process can be written as:

$$F(t) = C\ -\ c_R[R(t)] - c_I[I(t)] - c_P[P(t)]$$

The fit coefficient c_i proportional to the detachment cross-section with respect to the probe pulse whereas C is the offset value, associated with the photofragment yield produced by the pump laser only. Using the rate equation, we represent the concentration of each states as an exponential function with the rate constants as described below.

$$[R(t)] = 1 - \frac{1}{\sqrt{2\pi}w}\int_{-\infty}^{t} e^{-\frac{x^2}{2w^2}}dx = \frac{1}{2}\left(1 - \mathrm{erf}\left(\frac{t}{\sqrt{2}w}\right)\right),$$

$$\left(\mathrm{erf}(t) = \frac{2}{\sqrt{\pi}}\int_0^t e^{-x^2}dx\right)$$

$$[I(t)] = \frac{1}{\sqrt{2\pi}w}\int_{-\infty}^{t} e^{-\frac{x^2}{2w^2}} \cdot e^{-\frac{(t-x)}{\tau}}dx = \frac{1}{2}\left(1 + \mathrm{erf}\left(\frac{t}{\sqrt{2}w} - \frac{w}{\tau}\right)\right) \cdot e^{\frac{w^2}{2\tau^2} - \frac{t}{\tau}}$$

$$[P(t)] = 1 - [R(t)] - [I(t)]$$

w is the width of the cross-correlation determined to 43 fs ($FWHM = 2\sqrt{2ln2}w \approx 100\,fs$) from the time-resolved data of I_2^- in Fig. 2b. τ represents the reaction time within the photodetachable time-window, which indicates a slightly smaller values compared to the actual reaction rate. However, for simplicity, we will not distinguish between them in this context. The fitting function, *F(t)*, can be constructed by combining above equations with the coefficients, c_i. With τ and c_i as fitting parameters, transient data of the monomer anion in Fig. 3a were well-fitted.

$(CH_3NO_2)_2^- \rightarrow CH_3 + NO_2^-(CH_3NO_2)$

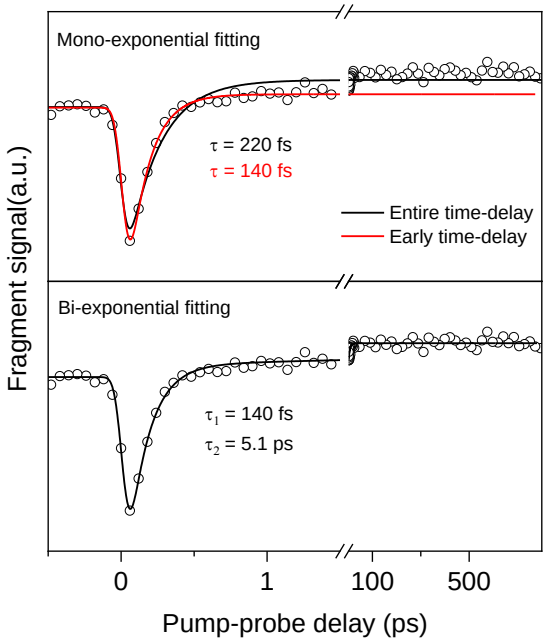

Fig. S3 TRPD spectra with $NO_2^-(CH_3NO_2)$ fragment of cryogenically cooled $(CH_3NO_2)_2^-$ with fitted functions.

The bond cleavage reaction of the dimer anion exhibits a similar transient feature to that of the monomer anion. However, the fitted function composed of mono-exponential functions deviates from experimental data (black line, Fig. S3). When fitting the early time delay data with a mono-exponential function, a good fit is obtained with a rate of 140 fs (red line). However, a slight deviation is observed at longer time delays, suggesting the existence of a minor dissociation pathway with a longer time scale. To explain bi-exponential behavior, we established new kinetic model for this reaction, expressed as:

$$R \overset{h\nu}{\rightarrow} I_1\,(NBS) \overset{\tau_1}{\rightarrow} P\,(NO_2^-(CH_3NO_2))$$

$$\overset{\tau_2}{\rightarrow} I_2 \overset{\tau_3}{\rightarrow} P\,(NO_2^-(CH_3NO_2))$$

According to the basic kinetics, for the existence of the picosecond-scale time constant, a portion of NBS population must transition to the intermediate state (I_2) where fragmentation occurs slowly. Therefore, it can be assumed that $\tau_1 < \tau_2$ and $\tau_1 \ll \tau_3$, and using this assumption, the populations of each anion species can be expressed according to the above kinetic model as follows:

$$[R(t)] = 1 - \frac{1}{\sqrt{2\pi}w}\int_{-\infty}^{t} e^{-\frac{x^2}{2w^2}}dx = \frac{1}{2}\left(1 - \mathrm{erf}\left(\frac{t}{\sqrt{2}w}\right)\right)$$

$$[I_1(t)] = \frac{1}{\sqrt{2\pi}w}\int_{-\infty}^{t} e^{-\frac{x^2}{2w^2}} \cdot e^{-\frac{(t-x)}{\tau_{NBS}}}dx = \frac{1}{2}\left(1 + \mathrm{erf}\left(\frac{t}{\sqrt{2}w} - \frac{w}{\tau}\right)\right) \cdot e^{\frac{w^2}{2{\tau_{NBS}}^2} - \frac{t}{\tau_{NBS}}}$$

$$\left(\frac{1}{\tau_{NBS}} = \frac{1}{\tau_1} + \frac{1}{\tau_2}\right)$$

$$[I_2(t)] = \begin{cases} \frac{\tau_1}{\tau_1 + \tau_2}(1 - [R(t)] - [I_1(t)]) & (t < 0) \\ \frac{\tau_1}{\tau_1 + \tau_2}(1 - [R(t)] - [I_1(t)]) \cdot e^{-\frac{t}{\tau_3}} & (t \geq 0) \end{cases}$$

$$[P(t)] = \begin{cases} \frac{\tau_2}{\tau_1 + \tau_2}(1 - [R(t)] - [I_1(t)]) & (t < 0) \\ \frac{1}{\tau_1 + \tau_2}(1 - [R(t)] - [I_2(t)]) \cdot (\tau_2 + \tau_1 \cdot \left(1 - e^{-\frac{t}{\tau_3}}\right) & (t \geq 0) \end{cases}$$

$$F(t) = C - c_R[R(t)] - c_{I_1}[I_1(t)] - c_{I_2}[I_2(t)] - c_P[P(t)]$$

However, this function has too many parameters for fitting. To reduce the number of parameters, the term [$I_2(t)$] and [$P(t)$] are expanded and reorganized. Since $(1 - [R(t)] - [I_1(t)])$ operates on the timescale of τ_1 and $(1 - e^{-\frac{t}{\tau_3}})$ operates on the timescale of τ_3, they are separated as follows:

$$c_{I_2}[I_2(t)] + c_P[P(t)]$$

$$= \frac{\tau_1 c_{I_1} + \tau_2 c_P}{\tau_1 + \tau_2} \cdot (1 - [R(t)] - [I_1(t)]) + \frac{\tau_1\left(c_P - c_{I_2}\right)}{\tau_1 + \tau_2} \cdot (1 - e^{-\frac{t}{\tau_3}})$$

The parameters of this equation can be combined into two new parameters, C_{I_2} and C_P, resembling the equation established for the monomer anion but with an additional single exponential function.

$$F(t) = C - c_R[R(t)] - c_{I_1}[I_1(t)] - C_{I_2}[1 - R(t) - I_1(t)] - C_P(1 - e^{-\frac{t}{\tau_3}})$$

This function fits the experimental data well, with τ_{NBS} at 140 fs and τ_3 at 5.1 ps. The obtained time constants are in line with the kinetic model established earlier, indicating the presence of pathway dissociating into the picosecond scale via an intermediate state, aside from the rapid dissociation channel. The ratio of NO_2^- (CH_3NO_2) fragmentation via this intermediate state can be approximately estimated using the assumption $\tau_1 \ll \tau_3$ as:

$$R \rightarrow I_1 \rightarrow I_2 \; pathway \; ratio = \frac{C_P - C_{I_2}}{C_P - c_{I_1}} = 0.048$$

$(CH_3NO_2)_2^- \rightarrow CH_3NO_2^- + CH_3NO_2$ and $(CH_3NO_2)_2^- \rightarrow CH_3 + NO_2^- + CH_3NO_2$

Both reaction channels are two-step processes, composed of sub-picosecond first step followed by a few hundred femtoseconds of a second step.

$$R \overset{h\nu}{\rightarrow} I_1 \, (NBS) \overset{\tau_1}{\rightarrow} I_2 \overset{\tau_2}{\rightarrow} P$$

With the assumption that τ_2 is much larger than τ_1, the transient equation can be derived simply as:

$$[R(t)] = 1 - \frac{1}{\sqrt{2\pi}w}\int_{-\infty}^{t} e^{-\frac{x^2}{2w^2}}dx = \frac{1}{2}\left(1 - \mathrm{erf}\left(\frac{t}{\sqrt{2}w}\right)\right), \quad \left(\mathrm{erf}(t) = \frac{2}{\sqrt{\pi}}\int_0^t e^{-x^2}dx\right)$$

$$[I_1(t)] = \frac{1}{\sqrt{2\pi}w}\int_{-\infty}^{t} e^{-\frac{x^2}{2w^2}} \cdot e^{-\frac{(t-x)}{t_1}}dx = \frac{1}{2}\left(1 + \mathrm{erf}\left(\frac{t}{\sqrt{2}w} - \frac{w}{t_1}\right)\right) \cdot e^{\frac{w^2}{2{t_1}^2} - \frac{t}{t_1}}$$

$$[I_2(t)] = \begin{cases} (1 - [R(t)] - [I_1(t)]) & (t < 0) \\ (1 - [R(t)] - [I_1(t)]) \cdot (e^{-\frac{t}{t_2}}) & (t \geq 0) \end{cases}$$

$$[P(t)] = \begin{cases} 0 & (t < 0) \\ \left(1 - e^{-\frac{t}{t_2}}\right) & (t \geq 0) \end{cases}$$

$$F(t) = C - c_R[R(t)] - c_{I_1}[I_1(t)] - c_{I_2}[I_2(t)] - c_P[P(t)]$$

Every function obtained in this chapter fits well with the experimental results, and the determined parameters are consistent with the actual reaction mechanism. For instance, the fit coefficients, c_i, proportional to the detachment cross-section, are in line with the trends of electron binding energies of anionic states obtained through either experiments or theoretical calculations. Also, the rapid dissociation at the repulsive potential due to fast internal conversion consistently occurs on the 140 fs, while cluster decomposition driven by vibrational energy consistently occurs on the order of several hundred picoseconds.

4. Kinetic Principles

When the reaction proceeds in two different competitive pathways, $\begin{cases} R \xrightarrow{k_1} P_1 \\ R \xrightarrow{k_2} P_2 \end{cases}$, rate equation can be described as:

$$-\frac{d[R]}{dt} = (k_1 + k_2)[R], \qquad \frac{d[P_1]}{dt} = k_1[R], \quad \frac{d[P_2]}{dt} = k_1[R]$$

By solving this differential equation, we can obtain the following solution.

$$[\mathrm{A}] = [A]_0 e^{-(k_1+k_2)t}$$

$$[P_1] = \frac{k_1}{k_1 + k_2}[A]_0(1 - e^{-(k_1+k_2)t})$$

$$[P_2] = \frac{k_2}{k_1 + k_2}[A]_0(1 - e^{-(k_1+k_2)t})$$

According to the equation, the growing rates of the products from two competitive reactions are expressed as the sum of each reaction rate, and the final concentration ratio follows the ratio of each reaction rate. In the case of the nitromethane dimer anion, when excited with a 1.57 eV photon, the competition of two fragment channels, $CH_3NO_2^-$ and $NO_2^-(CH_3NO_2)$, can be attributed to competitive internal conversion to the D_0^* and σ_{CN}^* states, respectively. The ratio of the two fragment yields at $h\nu$ = 1.57 eV obtained from the nanosecond photofragment action spectrum, $[NO_2^-(CH_3NO_2)]/[CH_3NO_2^-]$, is ~ 7.4. By assuming the NBS → D_0 transition is completely led to cluster decomposition, the measured lifetime of NBS, 80 fs, can be deconvoluted as 90 fs and 670 fs, for the internal conversion rates into the D_0^* and σ_{CN}^* states, respectively.

5. Time-Resolved Dynamics Extracted from the Fitting Process

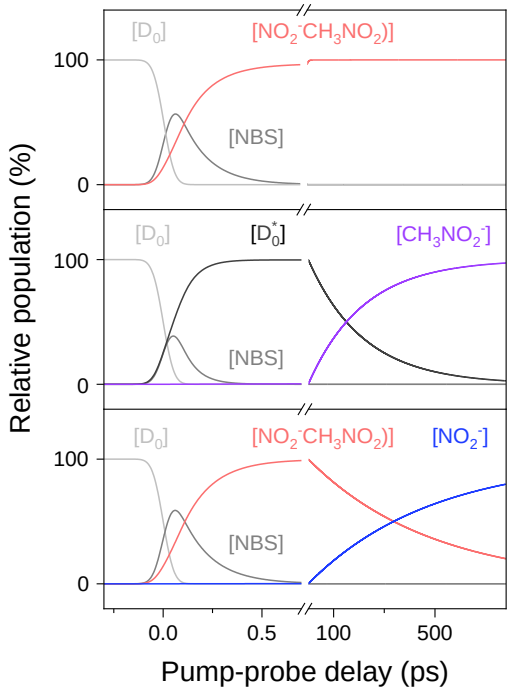

Fig. S4 Reaction dynamics showing the temporal changes of the anionic species extracted from the fits to the experiment for the C-N bond cleavage from $(CH_3NO_2)_2^-$ (Top), the cluster decomposition from $(CH_3NO_2)_2^-$ (middle), or the combination of those from $(CH_3NO_2)_2^-$ (bottom).

6. References

(1) An, S.; Kim, D.; Kim, J.; Kim, S. K., Excited-state chemistry of the nitromethane anion mediated by the dipole-bound states revealed by photofragment action spectroscopy. *Chemical Science* **2023,** 14 (43), 12231-12237.

(2) Adams, C. L.; Schneider, H.; Ervin, K. M.; Weber, J. M., Low-energy photoelectron imaging spectroscopy of nitromethane anions: Electron affinity, vibrational features, anisotropies, and the dipole-bound state. *The Journal of Chemical Physics* **2009,** *130* (7), 074307.

(3) Compton, R. N.; Jr., H. S. C.; Desfrançois, C.; Abdoul-Carime, H.; Schermann, J. P.; Hendricks, J. H.; Lyapustina, S. A.; Bowen, K. H., On the binding of electrons to nitromethane: Dipole and valence bound anions. *The Journal of Chemical Physics* **1996,** *105* (9), 3472-3478.

(4) Ervin, K. M.; Ho, J.; Lineberger, W. C., Ultraviolet photoelectron spectrum of nitrite anion. *The Journal of Physical Chemistry* **1988,** *92* (19), 5405-5412.

(5) Pruitt, C. J. M.; Albury, R. M.; Goebbert, D. J., Photoelectron spectroscopy of nitromethane anion clusters. *Chemical Physics Letters* **2016,** *659*, 142-147.

(6) Lu, Y.; Tang, R.; Zhang, R.; Ning, C., Probing Isomerization Dynamics via a Dipole-Bound State. *The Journal of Physical Chemistry Letters* **2022,** *13* (37), 8711-8716.